

To be published in Applied Optics:

Title: Achromatic optical elements

Authors: Anatoly Smolovich

Accepted: 16 June 2006

Posted: 19 June 2006

Doc. ID: 67247

Published by

OSA

Achromatic optical elements

Anatoly M. Smolovich

Scientific-Technological Center of Unique Instrumentation, Russian Academy of Sciences,

Butlerova 15, Moscow 117342, Russia

Institute of Radioengineering and Electronics (IRE), Russian Academy of Sciences,

Mokhovaya 11-7, Moscow 125009, Russia, petersmol@mtu-net.ru

The principles of wavefront reconstruction by means of a geometric-optical reflection of radiation from surfaces of interference fringe maxima are discussed. The optical elements based on these principles should be achromatic. Two methods of the optical elements design are proposed. The first method is direct holographic recording of the interference fringe structure containing only a few periods. The second method is a combination of the measurement of the object wavefront shape with digital holography methods.

OCIS codes: 090.0090, 090.1760, 090.1970, 090.2890, 100.5090

1. Introduction

Holographic methods allow recording and then reconstructing of an object wavefront ¹. The holographic mechanism of reconstruction is based on diffraction of reconstructing radiation by the recorded interference fringe structure. Just the local fringe period of this structure contains the information about the object wavefront. The reconstructed wavefront will be identical to the object one only if the reconstructing radiation wavelength is equal to the recording one. If it is not the case the reconstructed wavefront will have a magnification degree related to the wavelength change. In addition aberrations will

take place ². Therefore a wide spectrum band radiation cannot be used for conventional holographic reconstruction. Two types of holograms allowing white-light reconstruction were suggested: Denisyuk (also called Lippman-Bragg) hologram ³ and Benton (also called rainbow) hologram ⁴. However, in Denisyuk holography only a small part of wide-spectrum radiation with wavelength lying within a hologram spectral selectivity band actually interacts with a hologram. In Benton holography radiation with a wavelength different from the recording one propagates below or above observer's eyes. Therefore in both cases the most of wide-spectrum radiation does not actually take part in reconstruction.

There is another mechanism of wavefront reconstruction, which has been proposed by Denisyuk ⁵. It is based on a geometric-optical (GO) reflection of reconstructing radiation from surfaces with constant phase differences (SCPD) between the object and reference waves used to record the interference fringe structure in the medium bulk. Although the GO reconstruction mechanism was proposed for holography, it differs significantly from conventional holographic reconstruction and is of independent interest ^{6,7}. The most interesting property of GO wavefront reconstruction is that it is an achromatic one. This achromatic reconstruction is similar to light reflection from so-called "magic mirrors" – bronze mirrors produced 2000 years ago in ancient China ^{8,9}. Such a "magic mirror" forms an image on a distant wall when the Sun shines on the mirror. This is due to local irregularities of a reflecting surface acting as a concave or convex mirror. Some years ago a "magic mirror" or Makyoh (Ma-kyoh means "magic mirror" in Japanese) concept has been found to be useful for testing of mirror-like surfaces, such as semiconductor wafers, and detecting flaws induced by wafer slicing and polishing ¹⁰⁻¹³.

Denisyuk holography ⁵ together with Lippman photography ¹⁴ are also connected with further kinoform development. First, Stetson discussed the idea of achromatic wavefront reconstruction by alone isolated SCPD ¹⁵. Then Sheridan noticed that adjacent surfaces of hologram interference fringe maxima are nearly identical in shape ¹⁶ and used this fact in the development of a blazed hologram. The blazed hologram was recorded on a photoresist layer in reflection geometry. The developed photoresist surface contains areas with continuously varying microrelief related to parts of interference fringe maximum surfaces. These areas are divided by relief jumps due to transition from some interference fringe

maximum surface to the adjacent one. Later a computer generated optical element called kinoform was suggested¹⁷. In its reflection version the kinoform surface relief is similar to the blazed hologram surface relief obtained in¹⁶. However, in both cases the optical element operates correctly only for the design wavelength. This wavelength provides a 2π -phase jump at each boundary between zones with continuously varying surface relief. Later diffractive optical elements with a phase jump equaled to $2\pi M$ (where M is integer >1) were developed¹⁸⁻²⁷. These elements are known as multiorder²⁰ or harmonic²¹ diffractive lenses and also as deep relief kinoforms¹⁹. Multiorder diffractive lenses have some benefits in spectral properties¹⁸⁻²⁰ but they are not fully achromatic.

Thus achromatic optical elements are still of practical interest. They can be useful for operating with incoherent radiation and also with ultrashort laser pulses, which have a wide spectrum. Two types of the achromatic optical elements are analyzed in this paper. The first one is a volume optical element obtained by direct holographic recording of the interference fringe structure containing only a few periods. The second one is a surface-relief optical element obtained by a combination of physical field characteristic measurements with digital holography methods. Possible applications of proposed optical elements are listed in Conclusions.

2. Basic principles

Let us consider the interference between the object and reference monochrome waves in some region of space where both waves can be regarded as GO waves. Under these conditions the object and reference fields can be wrote as $A_O(\mathbf{r}) \exp[ikL_O(\mathbf{r})]$ and $A_R(\mathbf{r}) \exp[ikL_R(\mathbf{r})]$ accordingly, where $L_O(\mathbf{r})$ and $L_R(\mathbf{r})$ are the eikonals of the waves, $A_O(\mathbf{r})$ and $A_R(\mathbf{r})$ are the amplitude functions, \mathbf{r} is the position vector, $k=2\pi/\lambda$ is the wave number, and λ is the radiation wavelength. The intensity of the interference field of these waves is given by the expression:

$$A_O^2(\mathbf{r}) + A_R^2(\mathbf{r}) + 2A_O(\mathbf{r})A_R(\mathbf{r})\cos\{k[L_R(\mathbf{r}) - L_O(\mathbf{r})]\}. \quad (1)$$

The amplitude functions of GO waves satisfy the condition²⁸ $|\nabla A(\mathbf{r})|/A(\mathbf{r}) \ll k$. Then the surfaces of

constant intensity in (1) are defined by the condition of constant cosine argument in (1):

$$L_R(\mathbf{r}) - L_O(\mathbf{r}) = p, \quad (2)$$

where p is constant for a given surface of constant phase difference (SCPD). Suppose that the GO reconstructing wave $A_R(\mathbf{r}) \exp[ikL_R(\mathbf{r})]$, (where the wave number $k' = 2\pi/\lambda'$ may differ from k) is geometric-optically reflected by SCPD. Then the phase $k' L_{refl}(\mathbf{r})$ of the reflected wave on the surface (2) coincides with the phase of the incident wave²⁸:

$$k' L_{refl}(\mathbf{r}) = k' L_R(\mathbf{r}). \quad (3)$$

From (2) and (3) we obtain:

$$L_{refl}(\mathbf{r}) = L_O(\mathbf{r}) + p, \quad (4)$$

i.e., the eikonal of the object wave is reconstructed up to an additive constant for arbitrary k' . This also implies that the wavefront surface $L_O(\mathbf{r}) = const$ is achromatically reconstructed, or in other words, it does not depend on the wavelength of reconstructing light.

Under the same conditions a thin conventional hologram produces the field, which can be expressed as a sum of two terms¹:

$$A_O(\mathbf{r})A_R^2(\mathbf{r})\exp\{i[(k' - k)L_R(\mathbf{r}) + kL_O(\mathbf{r})]\} + A_O(\mathbf{r})A_R^2(\mathbf{r})\exp\{i[(k' + k)L_R(\mathbf{r}) - kL_O(\mathbf{r})]\}, \quad (5)$$

where the first and second terms correspond to the principal and conjugate images respectively. The wave corresponding to the first term has the eikonal

$$(\lambda'/\lambda) L_O(\mathbf{r}) + (1 - \lambda'/\lambda) L_R(\mathbf{r}) \quad (6)$$

Therefore the object wave eikonal will be reconstructed only if $\lambda' = \lambda$. For an arbitrary λ' expression (6) describes dispersion. For plane waves it leads to the grating formula, and for spherical waves it gives the expression obtained in². So, the waves reconstructed by the GO (eq. (4)) and conventional diffraction mechanisms (eq. (6)) are different for $\lambda' \neq \lambda$.

The following simple examples show the difference between reconstruction by reflection from SCPD and ordinary holographic reconstruction. In the simplest case of the plane object and reference waves, holographic reconstruction leads to reconstructing wave diffraction by a grating with a constant period; and reconstruction by reflection (GO reconstruction) results in the reconstructing wave reflection by a plane mirror. If the object wave is spherical, corresponding structures are a Fresnel zone plate and a parabolic mirror. In general the structure of SCPD is a mirror with a complicated curvature. The effect of GO wavefront reconstruction allows us to reconstruct a non-distorted wavefront by radiation with a wavelength different from the one used for recording. For example, this effect allows the use of radiation with wide spectrum band for wavefront reconstruction, where all spectral components (in the band of the hologram spectral selectivity) will actually take part in reconstruction, which is not the case in conventional holograms allowing white-light reconstruction^{3,4}.

3. Volume achromatic optical elements recorded by ultrashort pulses

An ordinary volume hologram contains parts of constant refractive index surfaces, which form a periodic structure due to a great number of such surfaces. Note that in practice, a volume hologram usually is a flat slab with a thickness of a few to tens of microns and with a lateral size of a few to tens of centimeters. A two-dimensional cross section of an ordinary reflection volume hologram is shown in Fig. 1a. The length of a periodic structure along the surface usually exceeds by several orders a size of each part of SCPD inside the slab. Hence the diffraction mechanism of wavefront reconstruction dominates upon the GO mechanism²⁹. This is confirmed by dispersion presence during reconstruction of ordinary reflection volume holograms that can be experimentally observed. Since a reconstructed beam can be observed only for a wavelength varying within a spectral selectivity band of a hologram, a large increase in hologram thickness makes this observation impossible for waves, which differ significantly from Bragg condition. At the same time, in case of Bragg reconstruction the diffraction and GO images are identical²⁹. To observe achromatic GO reconstruction, the number of surfaces of interference maxima recorded in the bulk must be decreased while the medium thickness is increased (Fig. 1b). We obtained in^{29, 30} for

the hologram recorded on a flat slab with thickness T by two short pulses with the duration equal to τ having plane wavefronts and propagating in opposite directions the following criterion of the GO reconstruction regime: $T \cos \psi \gg \tau c$, where ψ is an angle between the grating vector and the normal to the plate and c is the speed of light inside recording medium. The criterion was obtained by using the classical Gabor-Stroke approach³¹. The GO reflective hologram operates like a dielectric mirror. It does not have wavelength dispersion but it has wavelength/spectral selectivity.

The effect was experimentally observed using femtosecond-pulse sapphire titanate laser with an argon ion laser pump for recording^{7, 29, 32}. The radiation wavelength was varied in the range 780-830 nm. The pulses duration was equal to 40 fs and the pulses repetition frequency was equal to 80 MHz with average power of 200mW. The recording scheme is shown in Fig. 3. Since the standard photographic materials used in holography are typically 6-12 μm thick we used specially made materials of greater thickness. They are prepared from the silver halid emulsion "IAE opposed-type" developed at the Kurchatov Institute Russian Science Center and were characterized by a resolving power of 5000 lines per mm. The emulsions were up to 300 μm thick. The refractive index of the exposed emulsion after processing varied only in the pulse interference zone. The remaining volume of the illuminated emulsion was uniformly exposed within the beam width. The reconstruction band shifted to wavelengths of the order of 600 nm due to the photographic layer shrinkage during processing. A dye laser with wavelength tuning from 580 to 630 nm was used for reconstruction. The reconstructed beam was observed in a reflective geometry on a diffuse screen placed about 4 m from the photographic plate. The spectral selectivity of the structure recorded with the pulsed radiation made it possible to observe the reconstructed beam with a smooth variation of the wavelength of the radiation from 585 to 607 nm. Within this variation the spot produced on the screen by the reconstructed beam did not move, i.e., the direction of propagation of the reconstructed beam did not change. At the same

time, for the structure recorded with the continuous radiation under the same conditions, the spot on the screen moved by 6 cm. These facts prove that the GO mechanism of reconstruction but not the diffraction mechanism operates for structures recorded with femtosecond pulses.

4. Surface-relief optical elements

The achromatic hologram discussed in the previous section contains several SCPDs. However, for wavefront reconstruction only one SCPD is enough. Such a surface is not easy to make. In this section we suggest several methods for this.

First, a hologram with a surface relief is recorded in reflection geometry. The scheme of recording is similar to the one shown in Fig. 2. The only difference is that now recording can be done by continuous waves. The recording plate contains a photoresist layer. After its development a photoresist surface would have a serrated relief (Fig. 3a) as it was first obtained in ¹⁶. Each relief groove has a low-pitched part u_i corresponding to some SCPD (w_i). Within this part the relief depth varies continuously. The relief jump a_i between grooves corresponds to a transition from that SCPD (w_i) to the adjacent one (w_{i+1}). This relief shape is similar to the shape of reflection kinoform ¹⁷. The neighbor surfaces of the hologram interference maxima have shapes very similar to each other. Therefore cancel the relief jumps allows one to obtain a surface with a continuous variation of the profile, which is very close to the shape of the SCPD. The following operations should be performed for that: 1) the shape of the relief hologram surface is measured by some type of profilometer, 2) the obtained data is transferred into a computer, 3) the data is processed to cancel the jumps of the relief depth. The resulting surface is shown in Fig. 3b. This method looks clear. However, the shape of the interference maximum surface is not the only factor determining the shape of the relief hologram groove. It also depends on the complicated surface processes during photoresist development. Below we propose some other methods, which are free from this drawback.

It is known from electromagnetic theory ³³ that a 3D field distribution can be found from its 2D

distribution on some surface. Different approaches can be used to do this: the wave equation, Fresnel-Kirchhoff integral, the geometric-optical approximation, etc. In practice, it is sufficient to measure the object field distribution on some region of the surface to determine the field in some volume domain near it. Thus the 3D phase function $\Phi(\mathbf{r})$ of the object field in this domain also will be found. For the case of the GO object field its eikonal will be equal to $\Phi(\mathbf{r})/k$. Let's suppose that the object field interferes with a virtual GO reference wave having eikonal $L_R(\mathbf{r})$. The equation describing SCPD is similar to equation (2) and can be expressed as:

$$L_R(\mathbf{r}) - \Phi(\mathbf{r})/k = p. \quad (7)$$

Let's suppose that a reflective optical element with a surface described by (7) is synthesized in some manner, and a reconstructing wave with an eikonal equaled to $L_R(\mathbf{r})$ is directed onto it. In this case, as it was shown in section 2, the object wavefront would be reconstructed regardless of the reconstructing wave wavelength. Different value of p in (7) corresponds to a different position of the optical element.

We can divide the production process of the optical element for the object wavefront reconstruction into the following stages:

1. Measurement of a 2D distribution of the object field on some surface.
2. Calculation of the 3D object field and the shape of SCPD corresponding to interference of the object field with the virtual GO wave having the eikonal equaled to the eikonal of the reconstructing wave.
3. Fabrication of the optical element.

At the first stage the most difficult is to measure phase distribution. It can be performed by some kind of wavefront sensors: interferometric, heterodyne, Hartmann, etc. Also for a phase measurement a subsidiary amplitude 2D-hologram can be recorded. This hologram should be scanned by microdensitometer connected to a computer. The easier way is to record the hologram onto a CCD-camera connected to a computer. The reference wave for the subsidiary hologram recording has absolutely no connection to the virtual reference wave at stage 2 and can be chosen from a spatial frequency minimizing condition. In principal, the first stage can be skipped. In this case, optical element

would be fully computer generated.

The second stage. During computer information processing some additional operations besides the ones mentioned above are possible. These operations can include, for example, modification of the directional diagram, exclusion of the redundant information, transformation of the image size, combination of the real object images with the synthesized ones, determination of the phase functions that are more convenient for a physical realization, etc. Note, that both reflective and refractive (transmitting) optical elements can be realized. In the case of transmitting optical element synthesis the relief groves depth should be increased by a factor of $2/(n-1)$ (where n is the material refractive index) with respect to the case of the reflecting optical element. Under these conditions both elements would produce the similar phase distribution.

At the third stage different fabrication technologies, such as various lithographic methods²¹, processing by focused ion beams²⁶, and diamond turning of a master followed by molding^{21,24} can be used. The latter two mentioned technologies can provide big amplitude of the relief depth variation.

However, if this amplitude is too big the problem can be solved by the following technique³⁴. An optical system proposed consists of two elements: a blazed element (BE) and a stepped element (SE). These optical elements are situated closely to each other and can be produced on the opposite sides of the same substrate as it is shown in Fig. 4. The surface of the BE is divided into zones similarly to kinoforms¹⁷. The relief depth varies continuously within every zone and has jumps at the boundaries between neighbor zones. The analogous jump in kinoforms corresponds to the optical pass length equaled to the design wavelength λ_0 for the traditional kinoforms and equaled to $M\lambda_0$, where M is integer, for the multiorder kinoforms¹⁸⁻²⁶. Contrary to this in the proposed optical system the jump value is not related to the wavelength and also can be varied within one optical element. This is similar to the optical elements with modulated

zone sizes suggested in ²⁷. The working surface of each step of the SE represents a part of a plane normal to the optical axis. Each step of the SE has the corresponding zone in the BE. These step and zone are situated oppositely to each other and have the same shape from the top. The differences of the optical path lengths between the neighbor steps of the SE have equal absolute value and the opposite sign with the phase jumps at the boundary between the corresponding zones of the BE (condition of phase jumps compensation). In the option when both BE and SE are transmitting this condition simply means that the value of the relief depth jump of the BE is equal to the height of the appropriate step of the SE. The optical element shown in Fig. 4 can be constructed by cutting a standard optical lens into zones and shifting them along the optical axis. Contrary to the known kinoform elements here we shift not only the parts of the spherical surface but also the parts of the rear plane surface. The optical element shown in Fig.4 will have the same wavelength dispersion of the focal length due to its material refractive index dispersion as the original lens. This is significantly less than analogous value for diffractive elements ¹⁸. The option when one of the optical elements is reflective is also possible. The obvious limiting condition for the system parameters is that any corresponding zone and step should be in near-field region: $l_i \ll D_i^2/\lambda$, where λ is the reconstructing wavelength, l_i is the average distance between i -th zone of the BE and the corresponding step of the SE and D_i is their width. However, even in this case edge diffraction at the boundaries between zones of the BE and at the boundaries between steps of the SE would produce some noise.

Finally we would like to suggest an optical system where the edge effects mentioned above are eliminated. The proposed optical system (Fig. 5) contains two smooth optical elements not divided into zones. The first optical element has a strong focal power (SFPE). As fabrication of such element is difficult its surface can have deviations from the design shape. These deviations are compensated by the second optical element with a weak focal power (WFPE). The second element is fabricated after additional measurements of the wavefront formed by the first element in the region where the second element is supposed to be placed. Fabrication of the element with a weak focal power is significantly

easier. There are several possible combinations of reflecting and transmitting options for the SFPE and the WFPE. This is similar to the optical system containing the BE and the SE considered above. However, for the optical system shown in Fig. 5 the option when the SFPE is reflecting and the WFPE is transmitting is preferred. In this case chromatic aberrations due to the dispersion of transmitting optical element would be minimal. On the other hand, in the option when both optical elements are transmitting traditional methods of material dispersion compensation can be used.

5. Conclusions

A new approach to optical elements design is developed. The approach is based on the principles of the object wavefront reconstruction by GO reflection of radiation from the SCPD. Two ways of optical element design are discussed. The first one is recording of a hologram by femtosecond laser pulses in a volume medium. The second one is a measurement of the object wavefront shape followed by computer processing of this information and fabrication of the optical element. This element operates as an optical equivalent of the SCPD. Achromatic optical elements can be interesting for the following possible applications:

- Achromatic compensators of the real aberrations in optical devices, which are caused by an inaccuracy of manufacturing of the optical device and/or its elements.
- Focusing of radiation from powerful incoherent sources. This can create an alternative to the industrial lasers in some applications.
- Development of lampshades and lighting lenses for automobile headlights or other lighting units.
- Achromatic phase conjugation.
- Generation of the same object wavefront in the other spectral band. For example, some invisible spectral band wavefront can be transferred into the visible one for visualization.

Finally, note that a two-dimensional analog of an achromatic optical element is also possible. In ³⁵ we demonstrated femtosecond holograms recorded in a planar optical waveguide. Computer generated waveguide optical elements also can be developed.

References

1. D. Gabor, "Microscopy by reconstructed wavefronts," Proc. Roy. Soc. A**197**, 457-484 (1949).
2. R.W. Meier, "Magnification and third-order aberrations in holography," J. Opt. Soc. Am. **55**, 987-992 (1965).
3. Yu.N. Denisyuk, "On the reflection of optical properties of an object in the wave field of the radiation scattered by it," Sov. Phys. Dokl. **7**, 543-545 (1962).
4. S.A. Benton, "Hologram reconstruction with incoherent extended sources," J. Opt. Soc. Am. **59**, 1545A (1969).
5. Yu.N. Denisyuk, "On the reflection of optical properties of an object in the wave field of the radiation scattered by it," Opt. Spectrosc.(USSR) **15**, 279-284 (1963).
6. I.N. Sisakyan and A.M. Smolovich, "Achromatic reconstruction of a wavefront", Sov. Tech. Phis. Lett. **17**, 16-17 (1991).
7. D.A. Dement'ev, A.L. Ivanov, O.B. Serov, A.M. Smolovich, A.G. Stepanov and S.V. Chekalin, "Achromatic reconstruction of the wave front femtosecond laser pulses," JETP Lett. **65**, 402-404 (1997).
8. Z.M. Zhang, "Optics in China: Ancient and Modern Accomplishshments," In *International Trends in Optics*, J.W. Goodman, ed. (Acad. Press, Boston, 1991), Vol.1., pp. 185-194.
9. Hideya Gamo, "Magic Mirrors: Optics, Technology and History," demonstration and Poster Session WXI at the OSA Annual Meeting, New Orleans, 17-20 Oct., 1983.
10. S. Hahn, K. Kugimiya, M. Yamashita, P.R. Blaustein, K. Takahashi, "Characterization of Mirror-Like Wafer Surfaces Using the Magic Mirror method," Journal of Crystal Growth **103**, pp. 423-432 (1990).

11. S. Hahn, K. Kugimiya, K. Vojtechovsky, M. Sifalda, M. Yamashita, P.R. Blaustein, K. Takahashi, "Characterization of Mirror-Polished SI Wafers and Advanced SI Substrate Structures Using the Magic Mirror Method," *Semiconductor Science Technology* **7**, A80-A85 (1992).
12. F. Riesz, "Geometrical optical model of the image formation in Makyoh (magic-mirror) topography", *J. Phys. D: Appl. Phys.* **33**, 3033-3040 (2000).
13. F. Riesz, "Makyoh topography: a simple yet powerful optical method for flatness and defect characterisation of mirror-like surfaces", in *Optical Micro- and Nanometrology in Manufacturing Technology*, Ch. Gorecki, A.K. Asundi, eds., Proc. SPIE **5458**, 86-100 (2004).
14. G. Lippman, "Sur la theorie de la photographie des couleurs simples et composees par la methode interferentielle," *Journal de Physique* **3**, 97-107 (1894).
15. K.A. Stetson, "What is a hologram," *Laser Focus* **3** (5), 25-29 (1967).
16. N.K. Sheridon, "Production of blazed holograms," *Appl. Phys. Letters*, **12** 316-318 (1968).
17. L.B. Lezem, P.M. Hirsch, and J.A. Jordan, "The Kinoform: A New Wavefront Reconstruction Device," *IBM J. Res. Develop.* **13**, 150-155 (1969).
18. M. Kovatchev and R. Ilieva, "Inphase optical processors. 1. Inphase structures in optical computing", Invited paper 12A1, in *Proceedings of Optical Computing '90*, (Kobe, Japan, 1990), pp. 389-396.
19. M. Kovatchev and R. Ilieva, "Diffractive, refractive optics or anything more? Comparative analysis and trends of development", *J. Mod. Optics* **43**, 1535-1541 (1996).
20. D. Faklis and G.M. Morris, "Spectral properties of multiorder diffractive lenses", *Appl. Optics* **34**, 2462-2468 (1995).
21. D.W. Sweeney and G.E. Sommargen, "Harmonic diffractive lenses", *Appl. Optics* **34**, 2469-2475 (1995).
22. S. Sinzinger and M. Testorf, "Transition between diffractive and refractive micro-optical components", *Appl. Optics* **34**, 5970-5976 (1995).

23. M. Rossi, R.E. Kunz and H.P. Herzig, "Refractive and diffractive properties of planar micro-optical elements", *Appl. Optics* **34**, 5996-6007 (1995).
24. C.G. Blough, M. Rossi, S.K. Mack, and R.L. Michaels, "Single-point diamond turning and replication of visible and near-infrared diffractive optical elements", *Appl. Optics* **36**, 4648-4654 (1997).
25. T.R. Sales and G.M. Morris, "Diffractive-refractive behavior of kinoform lenses", *Appl. Optics* **36**, 253-257 (1997)
26. Y. Fu and N.K.A. Bryan, "Investigation of diffractive-refractive microlens array fabricated by focused ion beam technology", *Opt. Eng.* **40**, 511-516 (2001).
27. T. Ammer and M. Rossi, "Diffractive optical elements with modulated zone sizes", *J. Mod. Optics* **47**, 2281-2293 (2000).
28. Yu. A. Kravtsov and Yu. I. Orlov, *Geometrical Optics of Inhomogeneous Media* (Springer-Verlag, Berlin, 1990).
29. S.V. Chekalin, D.A. Dement'ev, A.L. Ivanov, Y. A. Matveets, O.B.Serov, A. M. Smolovich and A. G. Stepanov, "Geometric-optical reconstruction of a wavefront", in *ICONO '98: Nonlinear Optical Phenomena and Coherent Optics in Information Technologies*, S.S. Chesnokov, V.P. Kandidov, N.I. Koroteev, eds., *Proc. SPIE*, **3733**, 452-458 (1999).
30. M. A. Cervantes and A.M. Smolovich, "Ultrashort pulse scattering by 3-D interference fringe structure", in *ICONO 2001: Ultrafast Phenomena and Strong Laser Fields*, V.M. Gordienko, A.A. Afanas'ev, V.V. Shuvalov, eds., *Proc. SPIE* **4752**, pp.66-73 (2002).
31. D. Gabor and G.W. Stroke, "The theory of deep holograms", *Proc. Roy. Soc.* **A304**, pp. 275-289 (1968).
32. S.V. Chekalin, D.A. Dement'ev, A.L. Ivanov, Yu.A. Matveets, O.B. Serov, A.M. Smolovich and A.G. Stepanov, "Geometric-optical reconstruction of a wavefront. Experimental realization with femtosecond laser pulses", *Optics Commun.*, **150**, 38-42 (1998).
33. M. Born and E. Wolf, *Principles of optics* (Pergamon Press, Inc., New York, 2nd ed., 1964).

34. I.N. Sisakyan, A.M. Smolovich, and V.A. Soifer, "Apparatus for radiation focusing", Russian Patent N. 1620973 (1990).
35. S.A. Aseyev, M. A. Cervantes, S.V. Chekalin, V.O. Kompanets Yu.A. Matveets, O.B.Serov, A.M. Smolovich, V.S. Terpugov, "Femtosecond holography in planar optical waveguides," in *Photon Echo and Coherent Spectroscopy 2005*, V.V. Samartsev, ed., Proc. SPIE **6181**, 274-281 (2006).

List of Figure Captions

Fig. 1. Two mechanisms of wavefront reconstruction: (a) – conventional volume holograms, (b) – proposed GO volume holograms.

Fig. 2. Scheme of hologram recording in reflection geometry.

Fig. 3. Determination of SCPD shape from relief hologram, a – relief hologram, b – surface with constant phase differences (SCPD).

Fig. 4. Blazed element (BE) and stepped element (SE) produced on the opposite sides of the same substrate.

Fig. 5. Optical system of two smooth optical elements not divided into zones: optical element with a strong focal power (SFPE) and optical element with a weak focal power (WFPE).

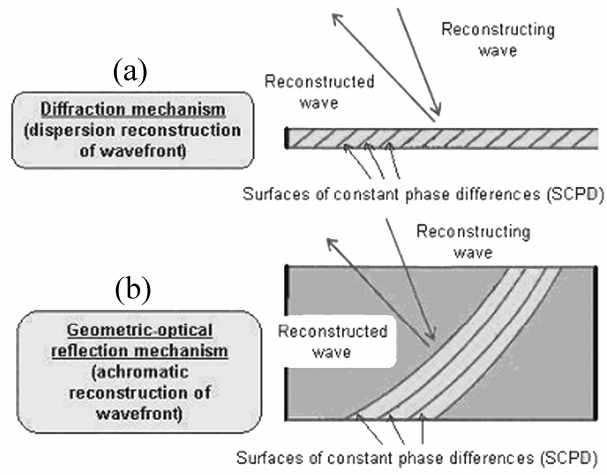


Fig. 1. Two mechanisms of wavefront reconstruction: (a) -conventional volume holograms, (b) - proposed GO volume holograms.

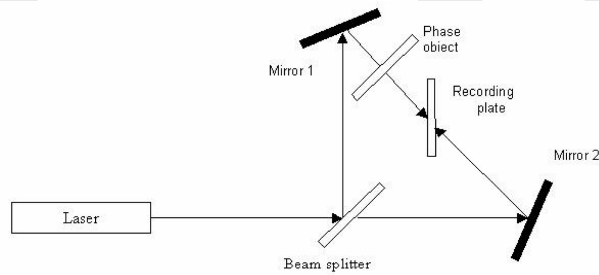


Fig. 2. Scheme of hologram recording in reflection geometry

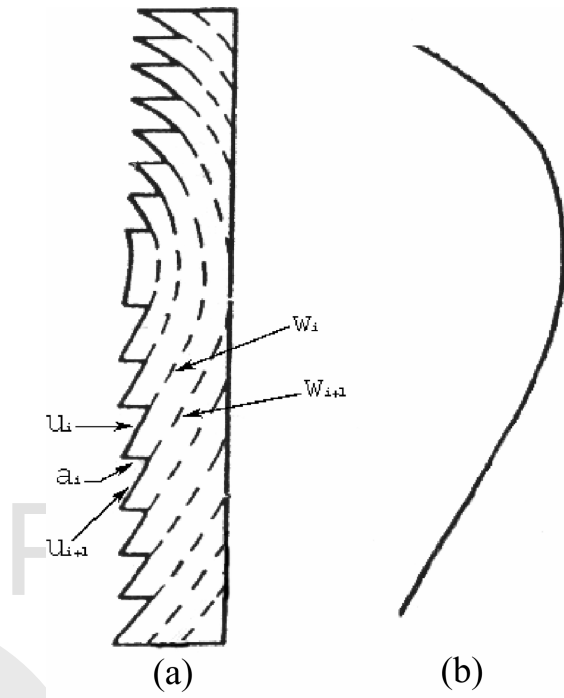


Fig. 3. Determination of SCPD shape from relief hologram, a – relief hologram, b - surface with constant phase differences (SCPD).

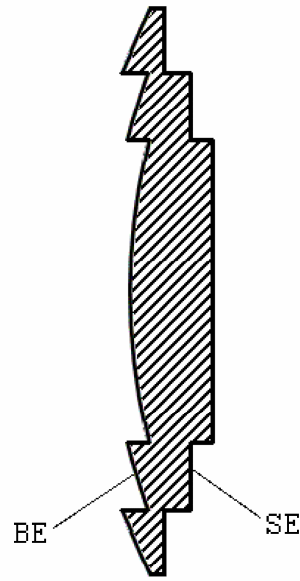


Fig. 4. Blazed element (BE) and stepped element (SE) produced on the opposite sides of the same substrate.

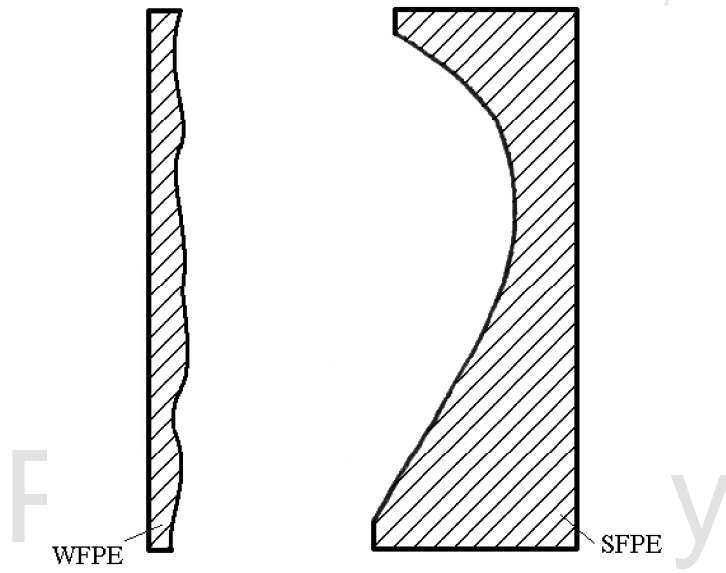


Fig. 5. Optical system of two smooth optical elements not divided into zones: optical element with a strong focal power (SFPE) and optical element with a weak focal power (WFPE).